Deuteron EDM Proposal: Search for a Permanent Deuteron Electric Dipole Moment at the 10^{-27} e·cm Level.

M. Aoki[15], M. Bai[4], G. Bennett[4], A. Bravar[4], H.N. Brown[4], G. Cantatore[16], A. Caracappa[4], R.M. Carey[3], P.T. Debevec[8], H. Denizli[1], F.J.M. Farley[4], C. Guclu[10], R. Hackenburg[4], S. Hoblit[4], H. Huang[4], K.P. Jungmann[7], M. Karuza[16], D. Kawall[12,13], B. Khazin[5], I.B. Khriplovich[5], B. Kirk[4], I.A. Koop[5], Y. Kuno[15], R. Larsen[4], D.M. Lazarus[4], L.B. Leipuner[4], C.P. Liu[7], V. Logashenko[3,5], M. Lowry[4], W.W. MacKay[4], K.R. Lynch[3], W. Marciano[4], W. Meng[4], J.G. Messchendorp[7], L. Miceli[4], J.P. Miller[3,*], W.M. Morse[4], G. Noid[9], C.J.G. Onderwater[7], Y. Orlov[6], C.S. Ozben[10], R. Prigl[4], S. Redin[5], S. Rescia[4], B.L. Roberts[3], G. Ruoso[11], T. Russo[4], A.M. Sandorfi[4], A. Sato[15], N. Shafer-Ray[14], Y. Shatunov[5], Y.K. Semertzidis[4,*], A. Silenko[2], E. Stephenson[9,*], R.G.E. Timmermans[7], C.E. Thorn[4], X. Wei[4], H.W. Wilschut[7], M. Yoshida[15]

1. **Abant Izzet Baysal University, Golkoy, BOLU 14280, Turkey**
2. **Belarusian State University, Belarus**
3. **Boston University,Boston, MA 02215, USA**
4. **Brookhaven National Laboratory, Upton, NY 11973, USA**
5. **Budker Institute of Nuclear Physics, Novosibirsk, Russia**
6. **Cornell University, Ithaca, NY 14853, USA**
7. **Kernfysisch Versneller Instituut, NL 9747 AA, Groningen, The Netherlands**
8. **University of Illinois, Urbana-Champaign, IL 61801, USA**
9. **Indiana University, Bloomington, IN 47408, USA**
10. **Istanbul Technical University, Maslak, Istanbul 34168, Turkey**
11. **Legnaro National Laboratories of INFN, Legnaro, Italy**
12. **University of Massachusetts, Amherst, MA 01003, USA**
13. **RIKEN-BNL, Upton, NY 11973, USA**
14. **University of Oklahoma, Norman, OK 73019, USA**
15. **Osaka University, Japan**
16. **University and INFN Trieste, Italy**

August 11, 2004

Requesting 4×10^{11} vector polarized, bunched, 0.7 GeV/c deuterons per 10 s cycle. Total running time 5000 hours.

* Spokesperson
miller@bu.edu, (617)353-2659; semertzidis@bnl.gov, (631)344-3881; stephens@iucf.indiana.edu, (812)855-5469.

Abstract

We are proposing a new method for measuring the electric dipole moment (EDM) of D^+, the bare deuteron nucleus directly, in a storage ring with a sensitivity of $10^{-27}\,\mathrm{e}\cdot\mathrm{cm}$. At this level the deuteron EDM is 10 to 100 times better than current EDM limits in terms of sensitivity to quark and gluon EDM, and the QCD θ parameter. It probes CP-violation at a range predicted by speculative theories beyond the standard model. The deuteron and neutron EDM searches are complementary and combined together they will provide severe constraint to the CP-violation sources.

Contents

1 Introduction **2**

2 Motivation of the Deuteron Electric Dipole Moment Experiment **4**

3 Concept of Experiment **6**
- 3.1 Overview of the Experimental Technique . . . 6
- 3.2 Polarimeter Design Considerations . . . 8
- 3.3 Statistical Accuracy . . . 10

4 Deuteron Storage Ring **12**
- 4.1 Lattice Design Considerations . . . 12
- 4.2 Polarization Lifetime (Spin Coherence Time) . . . 14
- 4.3 Non-Commutativity of Spin Rotations Imitating the EDM Rotation . . . 16
- 4.4 Magnetic/Electric Field Monitoring/Feedback Stabilization . . . 16

5 Systematic Errors **17**
- 5.1 Systematic Errors due to Electric and Magnetic Field Imperfections . . . 17
- 5.2 Polarimeter Systematic Errors . . . 21
- 5.3 Pickup Electrodes . . . 23

6 Management **23**
- 6.1 Group Organization and Responsibilities . . . 23
- 6.2 Outreach . . . 24

7 Cost and Schedule **25**
- 7.1 Conventional Facilities . . . 25
- 7.2 Accelerator Modifications . . . 25
- 7.3 Beam Transport . . . 26
- 7.4 Storage Ring . . . 26
- 7.5 Experimental Systems . . . 26
- 7.6 Totals . . . 26
- 7.7 R&D Request . . . 27

8 Conclusion **27**

1 Introduction

The quest for physics beyond the Standard Model (SM) currently represents a major effort in basic physics research. Since the Electric Dipole Moment (EDM) values predicted by most extensions to the SM are many orders of magnitude larger than those of the SM itself and close to present limits, EDM experiments have become very sensitive probes for new physics. Future searches will either locate an EDM or severely constrain SM extensions. Furthermore, a non-vanishing EDM is a violation of T and P symmetries, and under the assumption of CPT invariance would imply a new source of CP violation, perhaps shedding light on the puzzling baryon/anti-baryon asymmetry of the universe. Even if an EDM is found in another experiment, multiple observations will be needed to characterize the form of the CP violation. Indeed, EDM searches have already helped to shape our knowledge of fundamental particles and interactions for more than half a century. From the early, pioneering experiments on the neutron in the 1950s [1], limits on both neutron and atomic EDMs have been improved by many orders of magnitude. However, it is striking to note that so far, all sensitive searches have been performed on neutral systems. EDM limits on the charged constituents have been inferred with theoretical estimates.

In our proposed experiment, the EDM of D^+, the bare deuteron nucleus is probed, directly, using a storage ring technique which has the potential to increase the sensitivity of EDM measurements by another two orders of magnitude. Longitudinally polarized deuterons are first injected into a storage ring. During the storage time we probe the spin precession in both the "horizontal" and "vertical" directions by polarimetry, detecting deuterons scattered by solid carbon targets. For a particle at rest, an EDM couples to the electric field and a magnetic moment couples to the magnetic field. Since a relativistic particle in a magnetic storage ring feels both magnetic and electric fields in its rest frame, its spin precession vector will be modified by the presence of an EDM. This was recognized early on [2] and this method was applied to set limits on the muon EDM [3]. The EDM signal is a change in the "vertical" polarization with time given by

$$\Delta P_V = P \, \frac{\omega_{edm}}{\Omega} \, \sin(\Omega t + \theta_0), \qquad \Omega = \sqrt{\omega_{edm}^2 + \omega_a^2} \tag{1}$$

where P is the polarization of the particle beam, and ω_a, ω_{edm} are the precession frequencies arising from the magnetic and electric dipole moments, respectively. ω_a is the "horizontal" precession frequency measured in g-2 experiments. ω_{edm} is a "vertical precession" which would tip the usual g-2 precession out of the horizontal plane. In our experiment, we maximize the change in the "vertical" polarization during beam storage by applying a radial E-field [4, 5], and reduce ω_a by a factor of 10^7. Then $\Omega\, t < 1$ at all times up to 10 s, and, for small θ_0, the term $\sin(\Omega t + \theta_0) \simeq \Omega\, t$. Therefore $\Delta P_V(t) \simeq P\, \omega_{EDM}\, t$, i.e. cancelling ω_a to $\geq 10^7$ amplifies the maximum value of $\Delta P_V(t)$ by 10^7.

Our goal is to measure the deuteron EDM with a sensitivity of 10^{-27} e·cm. Of the best existing EDM measurements, the current limit on the neutron EDM is $6 - 10 \times 10^{-26}$ e·cm [6], that on the Thallium atom is $\simeq 10^{-24}$ e·cm (90% C.L.) [7] and that of the mercury atom is 2.1×10^{-28} e·cm (95% C.L.) [8]. The sensitivity level of each system depends on the details of the dynamics of the constituent charged particles. Screening by atomic electrons, for example, makes the mercury result a less sensitive limit for the neutron than the test on the neutron itself [9]. The deuteron EDM experiment at the 10^{-27} e·cm level is more sensitive than the above limits in restricting $\bar{\theta}$, the CP violating QCD vacuum angle, and quark EDMs by one to two orders of magnitude. Fig. 1 (from reference [10]) shows that a deuteron EDM experiment at the level of 3×10^{-27} e·cm, is more sensitive than any present EDM limit by one to two orders of magnitude for all SUSY parameters.

As the deuteron nucleus is an extended object, it has a finite polarizability and an externally

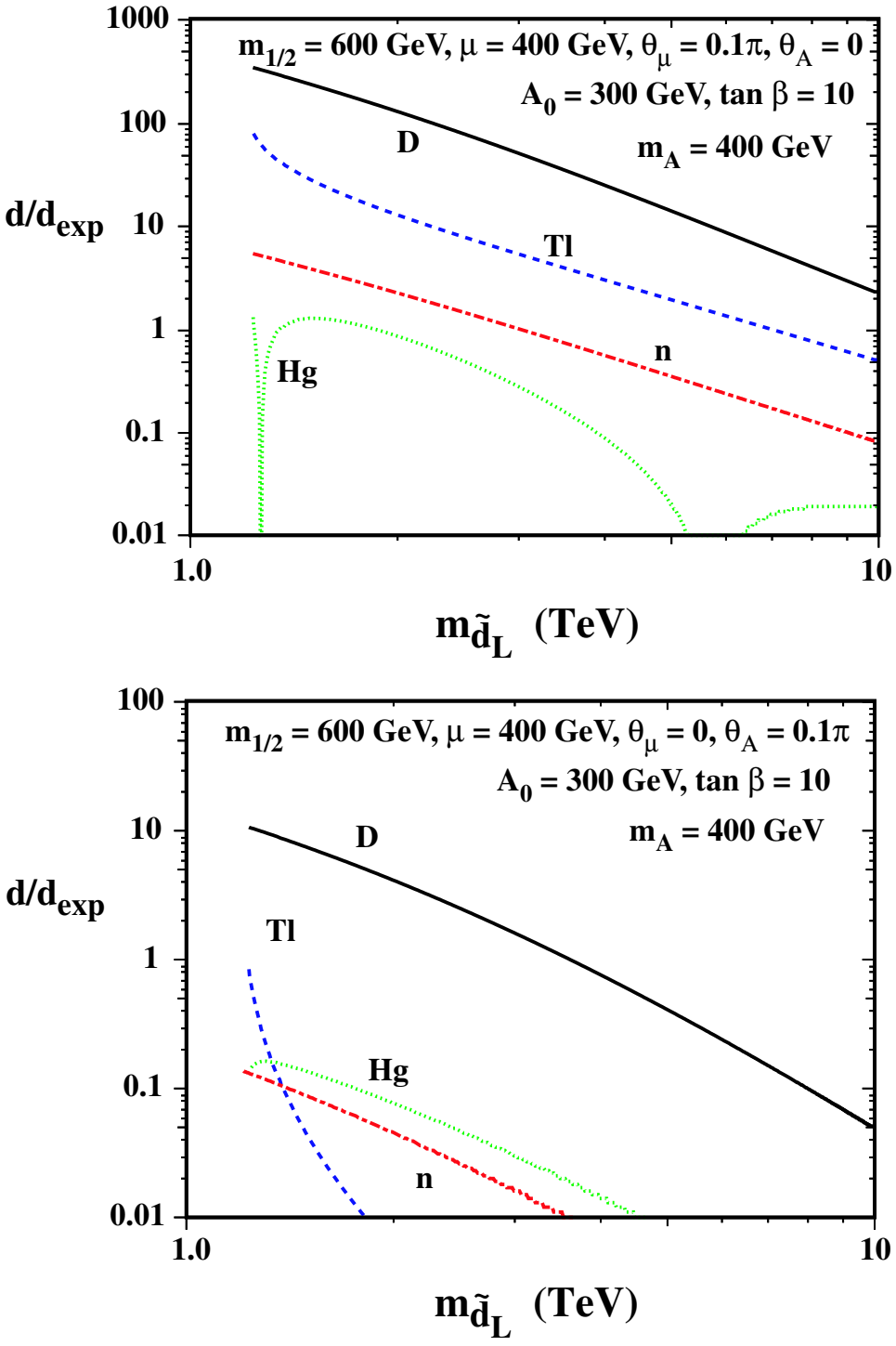

Figure 1: (From reference [10].) The EDMs of the deuteron (black), mercury (green), the neutron (red), and thallium (blue) as a function of the SUSY soft breaking scalar mass m_0, displayed in terms of the left-handed down squark mass. On top $\theta_A = 0$, $\theta_\mu = \pi/10$ and on bottom $\theta_A = \pi/10$, $\theta_\mu = 0$. The EDM is normalized to the experimental constraint in each case except for the deuteron where a limit of 3×10^{-27} e$\cdot$cm is assumed.

applied E-field will produce an EDM which we estimate to be less than $d_{\rm ind} < 10^{-29}$ e·cm. Since the induced EDM is parallel to the electric field, $\vec{d}_{\rm ind} \times \vec{E} = 0$, it produces no additional spin precession. In addition, the deuteron has a small electric quadrupole moment which will contribute to the spin motion. The resulting error, $\sigma_d < 10^{-30}\,{\rm e}\cdot{\rm cm}$, is negligible. Finally, our ultimate statistical error goal will require a large number of deuterons. Fortunately, high intensity, highly-polarized deuteron beams are readily available.

As in any precision measurement, there are a number of experimental challenges, here in both beam dynamics and in polarimetry. In order to obtain the long spin coherence times (> 10 s) required by our technique, sextupole magnets will be added at specific azimuthal locations in the magnetic lattice, and RF will be employed. To control the $g-2$ precession to 1 part in 10^7, the *relative* values of the magnetic and electric fields must be known at this same level. We will monitor them separately by measuring the $g-2$ precession angle of the deuteron beam itself and by using atomic and molecular beams. The effect of the most dangerous stray field, an average vertical electric field, is minimized by injecting deuterons clockwise (CW) and counter-clockwise (CCW) into the storage ring. This dual-injection scheme requires that we flip the magnetic field of 0.2 T while keeping the radial E-field the same.

The spin direction will be measured with polarimeters, which are available with high analyzing power in the momentum range of interest (0.7 GeV/c). The deuterons are scattered off carbon. The vertical component of the spin, which contains the EDM signal, leads to a measurable left-right asymmetry in the number of scattered particles.

The collaboration feels it has the experience with spin and beam dynamics to deal with these and many other systematic errors. Many of us faced similar problems of comparable difficulty on the muon $g-2$ experiment. The collaboration is also strong in the new components of the experiment, i.e. the use of deuteron polarimeters to analyze the spin components. Also it has been strengthened by the addition of members with significant experience in atomic and molecular beams required to measure the magnetic and electric fields and in Fabry-Perot interferometry that will be used to monitor the temporal stability of the electrostatic plates. The measurement of the deuteron EDM at BNL is anticipated to cost a little over \$30 M including BNL overhead and a 25% contingency and is expected to take data for two years, starting four years after the scientific approval.

2 Motivation of the Deuteron Electric Dipole Moment Experiment

The existence of an intrinsic EDM requires that the discrete symmetries P (parity) and T (time reversal) be violated. In the Standard Model, both symmetries are indeed violated. Hence, one should expect all states with spin, elementary particles and bound states, to possess EDMs. However, the violation of T (or CP) in the Standard Model is generally very small, resulting from high order quantum loops; thereby leading to EDM predictions many orders of magnitude beyond the sensitivity of ongoing or contemplated experiments. Therefore, the observation of any intrinsic EDM would represent the discovery of a new type of CP violation in nature, never seen before. Such a discovery would likely have a profound implications, since explaining the matter-antimatter asymmetry [11] of our universe appears to require a source of CP violation beyond the Standard Model.

Traditionally, the most sensitive EDM searches have involved the neutron or heavy atoms. In the case of atoms, their EDMs could result from intrinsic electron or nucleon EDMs as well as from CP violating interactions. The strategy is to first find any EDM and then use other states (with

positive or null EDM results) to unravel its source.

The deuteron is a new entry in the race to find an intrinsic EDM. This spin one bound state of a proton and neutron falls in between the neutron and heavy atoms in its complexity. Finding or significantly bounding the deuteron EDM would provide important complementary information to the neutron and atomic systems. In that regard, the ability to search for a deuteron EDM at the $10^{-27}\,\mathrm{e}\cdot\mathrm{cm}$ level by the method proposed here represents a major step forward in a new arena.

In evaluating the relative merits of a deuteron EDM experiment, several issues have to be addressed. How does its sensitivity (in this case $10^{-27}\,\mathrm{e}\cdot\mathrm{cm}$) compare with expected or planned neutron and atomic EDM experiments? Can a deuteron EDM discovery be consistent with existing neutron or atomic bounds? How complementary is the deuteron? The comparison of different EDM searches necessarily requires a model for the CP breaking physics. However, recent generic studies have shown that at the $10^{-27}\,\mathrm{e}\cdot\mathrm{cm}$ level, the deuteron EDM search is at least one to two orders of magnitude more sensitive than any current EDM limit. Furthermore, it is well within the predictions of specific SUSY models [10, 12, 13, 14].

The utility of a deuteron EDM measurement has been addressed by several recent studies. Here, we briefly outline results given by Khriplovich and Korkin [15] as well as Lebedev *et al.* [10] regarding the relative merits of different EDM measurements.

The deuteron EDM can be parameterized in terms of neutron and proton EDMs along with a nuclear bound state component,

$$d_D = d_n + d_p + d_D^{\mathrm{Nuclear}} \tag{2}$$

with each component primarily arising from some new CP-violating underlying physics. (Standard Model contributions are negligible.) The dominant nuclear contribution can be described as stemming from CP violating effective pion-nucleon "scalar" interactions:

$$\mathcal{L}_{\not CP} = \bar{g}^{(0)}_{\pi\mathrm{NN}}\bar{N}\tau^a N\pi^a + \bar{g}^{(1)}_{\pi\mathrm{NN}}\bar{N}N\pi^0 \tag{3}$$

where the $\bar{g}^{(I)}$ are derived from a more fundamental underlying theory such as supersymmetry. To simplify the discussion, we do not consider here the CP-odd πNN interaction with $\Delta I = 2$, where I is the isospin number. From those effective interactions, one finds

$$d_D^{\mathrm{Nuclear}} \simeq -1.2\,\bar{g}^{(1)}_{\pi\mathrm{NN}}\,\frac{e}{m_N} = -2.5\times 10^{-14}\,\bar{g}^{(1)}_{\pi\mathrm{NN}}\,\mathrm{e}\cdot\mathrm{cm} \tag{4}$$

Those same interactions also give rise to nuclear EDMs, d_n and d_p. So, for example, a QCD CP violating interaction

$$\mathcal{L}_{\not CP} = \bar{\theta}\,\frac{\alpha_s}{8\pi}\,G\tilde{G} \tag{5}$$

gives rise to (in leading log order)

$$d_n(\bar{\theta}) \simeq -d_p(\bar{\theta}) \simeq 3.6\times 10^{-16}\ \bar{\theta}\ \mathrm{e}\cdot\mathrm{cm} \tag{6}$$

which provides the bound

$$\bar{\theta} < 10^{-9} \tag{7}$$

From Eq. (6) and Eq. (2), the contribution to d_D through the neutron and proton would appear to have little sensitivity to $\bar{\theta}$. However, non-leading log contributions (isoscalar) to d_n and d_p combined with $\bar{g}^{(1)}_{\pi\mathrm{NN}}$ contributions due to $\pi-\eta$ mixing give

$$d_D(\bar{\theta}) \simeq -10^{-16}\ \bar{\theta}\ \mathrm{e}\cdot\mathrm{cm} \tag{8}$$

which is about $(-)$ 25% of d_n. So, a deuteron experiment at the $10^{-27}\,\mathrm{e}\cdot\mathrm{cm}$ level is sensitive to $\bar{\theta} \simeq 10^{-11}$ and provides complementarity to future d_n probes. It also provides the consistency check $d_n \simeq -3.6\, d_D$.

That level of sensitivity is generally true for d_D from other models. As an illustration, we consider the effects of quark electromagnetic and color EDMs, d_q and $\tilde{d}_q$, through

$$\mathcal{L}_{\not CP} = -\frac{i}{2}\sum_q \bar{q}\left(d_q \sigma_{\mu\nu} F^{\mu\nu} + \tilde{d}_q \sigma_{\mu\nu} G^{\mu\nu}\right)\gamma_5\, q \tag{9}$$

which leads to

$$d_D(d_q, \tilde{d}_q) \simeq 0.5(d_u + d_d) - 5.6e(\tilde{d}_u - \tilde{d}_d) - 0.2e(\tilde{d}_u + \tilde{d}_d) \tag{10}$$

That is to be compared with the neutron [16]

$$d_n(d_q, \tilde{d}_q) \simeq \left[\left(\frac{4}{3}d_d - \frac{1}{3}d_u\right) + 1.1e\left(\tilde{d}_d + \frac{1}{2}\tilde{d}_u\right)\right] \times 0.5 \tag{11}$$

Again, d_D and d_n are complimentary, testing different linear contributions of the quark dipole moments. Similar comparisons can be made with the sensitivity obtained from atoms such as Tl, Xe, and Hg. In some cases, such as Tl, the atoms are particularly sensitive to the electron EDM due to relativistic enhancement effects (e.g. $d_{\mathrm{Tl}} \simeq -600\ d_e$). However, the heavy atoms are generally not competitive with a $10^{-27}\,\mathrm{e{\cdot}cm}$ d_D sensitivity when it comes to $\bar{\theta}$ or quark dipole moment effects

$$\begin{aligned} d_{\mathrm{Tl}} &\simeq 7 \times 10^{-18}\,\bar{\theta}\ \mathrm{e}\cdot\mathrm{cm}, \\ d_{\mathrm{Xe}} &\simeq 1.4 \times 10^{-18}\,\bar{\theta}\ \mathrm{e}\cdot\mathrm{cm}, \\ d_{\mathrm{Hg}} &\simeq 1 \times 10^{-19}\,\bar{\theta}\ \mathrm{e}\cdot\mathrm{cm}. \end{aligned} \tag{12}$$

In summary, a deuteron EDM experiment with $10^{-27}\,\mathrm{e}\cdot\mathrm{cm}$ sensitivity is competitive with or in some cases better than forthcoming neutron and atomic EDM studies. Should an EDM be observed in any of those systems, the others will be critical in sorting out the underlying source of CP violation responsible.

3 Concept of Experiment

3.1 Overview of the Experimental Technique

We are proposing a new sensitive method of searching for the electric dipole moment of charged particles using a storage ring. The storage ring provides a clean environment with intense, highly polarized, and stable beams of low emittance. The dominant systematic errors for the traditional neutral particle EDM search techniques are absent, or highly suppressed.

First we discuss the problems inherent in the traditional neutral particle EDM experimental method, and then introduce the new storage ring method. The spin precession for a particle at rest, $\vec{v} = 0$, is:

$$\frac{d\vec{S}}{dt} = \mu\vec{S} \times \vec{B} + d\hat{S} \times \vec{E} \tag{13}$$

where the magnetic moment $\mu = ge/2mc$, and d is the electric dipole moment. For the neutron, e/m of the proton is used; and $g_n = -3.8$. Neutron EDM experiments have been ongoing since the

1950s [17]. The experiments have been performed in a weak magnetic field, typically 1 μT, and a strong electric field, typically 2 MV/m. The spin precession frequency is measured with the electric field parallel and anti-parallel to the magnetic field. A change in the measured spin precession frequency would be evidence for an EDM.

A systematic error can originate from any stray magnetic field, such as one caused by leakage currents from the electric field electrodes, which changes when the electric field is flipped. In a real neutral particle EDM experiment with $|\vec{v}| \ll c$, the spin precession is given by

$$\frac{d\vec{S}}{dt} = \mu\vec{S} \times \left(\vec{B} - \vec{v} \times \vec{E}\right) + d\hat{S} \times \left(\vec{E} + \vec{v} \times \vec{B}\right) \tag{14}$$

The $\mu(\vec{S} \times (\vec{v} \times \vec{E}))$ term represents a systematic error in the EDM search since this term, like the EDM precession term, changes sign when the electric field changes sign. Note that the $d(\hat{S} \times (\vec{v} \times \vec{B}))$ term increases the EDM signal, but it is negligible compared to the electric field term.

Next we discuss the situation for a relativistic particle in a storage ring [18] where there are both magnetic and electric fields. The spin precession due to the magnetic dipole moment is:

$$\frac{d\vec{S}}{dt} = \frac{e}{m}\vec{S} \times \left[\left(a + \frac{1}{\gamma}\right)\vec{B} - a\frac{\gamma}{\gamma+1}\left(\vec{\beta}\cdot\vec{B}\right)\vec{\beta} - \left(\frac{g}{2} - \frac{\gamma}{\gamma+1}\right)\frac{\vec{\beta}\times\vec{E}}{c}\right] \tag{15}$$

where $a = (g-2)/2$ is the anomalous magnetic moment. The spin precession due to the electric dipole moment is simply:

$$\frac{d\vec{S}}{dt} = d\left[\hat{S} \times \left(c\vec{\beta} \times \vec{B} + \vec{E}\right)\right] \ . \tag{16}$$

The $d\,\hat{S} \times \vec{E}$ term can be neglected in the above equation, since this change in the EDM signal is small compared to the magnetic field term. The spin precession due to the electric dipole moment is about the $\vec{\beta} \times \vec{B}$ vector.

For the simple case of $\vec{\beta}\cdot\vec{B} = \vec{\beta}\cdot\vec{E} = 0$, the precession of the spin direction, relative to the momentum direction, is given by $\vec{\omega} = \vec{\omega}_a + \vec{\omega}_{edm}$ where

$$\vec{\omega}_a = \frac{e}{m}\left[a\vec{B} + \left(\frac{1}{\gamma^2-1} - a\right)\frac{\vec{\beta}\times\vec{E}}{c}\right] \tag{17}$$

is the rotation about the vertical ($\vec{B}$-field direction) direction that arises because there is an anomalous part to the magnetic moment. The motion about the radial direction, for a spin one particle,

$$\vec{\omega}_{edm} = d\,\frac{c}{\hbar}\left(\frac{\vec{E}}{c} + \vec{\beta}\times\vec{B}\right) \tag{18}$$

comes from the torque produced on the EDM. The EDM signal is an increasing vertical polarization produced by a non-vanishing ω_{edm} precession. The change in the vertical polarization with time is

$$\Delta P_V(t) = P\,\frac{\omega_{edm}}{\Omega}\,\sin(\Omega t + \theta_0), \qquad \Omega = \sqrt{\omega_{edm}^2 + \omega_a^2} \tag{19}$$

where P is the polarization of the particle beam. Thus it behooves us to minimize ω_a, although for systematic error management ω_a should be small but not zero. This can be done by applying a radial electric field of magnitude

$$E_r = \frac{aBc\beta\gamma^2}{1 - a\beta^2\gamma^2} \simeq aBc\beta\gamma^2 \tag{20}$$

to cancel the $a\vec{B}$ contribution to ω_a in Eq. (17) [4, 5]. A sensitive EDM search requires large electric fields and particles with a small anomalous moment.

Unfortunately, there are no particles with $a = 0$. Leptons have $a \simeq 0.001$. The electron imposes difficulties using the storage ring technique since it generates a large amount of synchrotron radiation, which introduces an additional systematic error: an electron beam in a storage ring develops a polarization component along the direction of the magnetic field vector. The situation is much better for the muon since synchrotron radiation intensity falls as $1/m^4$. An LOI has been submitted to JPARC [19] for a muon EDM experiment at the level of $10^{-24}\,\mathrm{e}\cdot\mathrm{cm}$ statistical and $10^{-27}\,\mathrm{e}\cdot\mathrm{cm}$ systematic error. The statistical error is large because of the difficulty of obtaining a sufficient flux of stored muons; the muon beam derives from a secondary pion beam and is created with very large emittance. Its lifetime also limits the time for observing the EDM precession. The challenge of a MW proton beam creating an intense muon beam means that this experiment is at least one decade away from physical realization. Thus other cases that can reach the same level of sensitivity in a shorter time are preferred.

The deuteron is an ideal candidate. It has a small anomaly, $a = -0.143$. Intense, low-emittance beams with high polarization and efficient polarimeters are readily available. We are proposing here a search for the deuteron EDM with statistical error $< 10^{-27}\,\mathrm{e}\cdot\mathrm{cm}$ and systematic error $\simeq 10^{-27}\,\mathrm{e}\cdot\mathrm{cm}$.

The EDM systematic error due to a weak magnetic field induced by leakage currents from the electric field electrodes is negligible since the storage ring magnetic field is strong ($\simeq 10^{-1}$ T), not weak ($\simeq 10^{-6}$ T), as in the neutral beam EDM experiments. Furthermore, in the storage ring EDM search, the $\vec{v}\times\vec{E}$ precession term is not a systematic error, but rather a tool to control the $g-2$ precession rate to increase the statistical sensitivity to the EDM. In order to control systematic errors, the $g-2$ precession rate is varied, as discussed later.

We have extensively studied spin dynamics systematic errors [4]. We have found only one first-order spin dynamics systematic effect for the Storage Ring EDM experiment: if there is a non-zero average value for the vertical component of the electric field, $\langle E_V\rangle \equiv \langle\vec{E}\cdot\vec{B}\rangle/B \neq 0$, then the spin will precess about the radial direction:

$$\omega_{syst} \simeq \frac{\mu\langle E_V\rangle}{\beta c\gamma^2}. \tag{21}$$

This effect, relative to the EDM effect, changes sign when injecting beam clock-wise (CW) vs. counter-clockwise (CCW) into the ring. This can be seen from Eqs. (17) and (18). In going from CW to CCW, $\vec{\beta}\to-\vec{\beta}$, $\vec{B}\to-\vec{B}$, and $\vec{E}\to\vec{E}$, therefore $\vec{\omega}_a$, and thus ω_{syst}, changes sign, while ω_{edm} does not. Thus, conceptually, the EDM signal is separated from false signals in a comparison of the measured deuteron spin precession rates about the $\vec{\beta}\times\vec{B}$ direction when injecting CC vs. CCW. The ratio of the spin precession due to the vertical electric field to the EDM spin precession, which needs to be minimized in the design of the experiment, is given by

$$R = \frac{a\,\mu\langle E_V\rangle}{d\beta cE}\ . \tag{22}$$

We have chosen for a storage ring conceptual design $p_D = 0.7$ GeV/c or $\beta = 0.35$. A larger value of β would reduce the ratio R, however the ring cost would increase. A modest electric field value $E \simeq \pm 85\,\mathrm{KV}/5\,\mathrm{cm}$ results in $B \simeq 0.2$ T.

3.2 Polarimeter Design Considerations

A polarized ion source for spin-one deuteron beams changes the fraction, f_1, f_0, or f_{-1}, of the beam that is in each of the three magnetic substates away from the unpolarized values of $f_1 =$

$f_0 = f_{-1} = 1/3$. This can produce either a vector polarization ($p_Z = f_1 - f_{-1}$) and/or a tensor polarization ($p_{ZZ} = 1 - 3f_0$) with respect to the orientation of the quantization axis established by the magnetic field in the ion source. As tensor polarization may lead to systematic errors, p_{ZZ} is kept small by maintaining f_0 as close to 1/3 as possible. This limits the vector polarization to values where $|p_Z| < 2/3$.

The polarization of the circulating deuteron beam is best measured by colliding the deuterons with a target and observing reaction products generated through the action of the strong nuclear force. A thorough knowledge of the polarization components requires that we detect particles at a variety of angles (θ, ϕ) where θ is the polar angle measured from the momentum direction and ϕ is the azimuthal angle that starts from the left (facing along the beam momentum) in the $g-2$ precession plane and advancing in the clockwise direction. The orientation of the quantization axis is a result of the cumulative effect of the transport line and ring electromagnetic fields. Its orientation when it reaches the polarimeter target is specified by a second set of spherical angles (ξ, ψ) with respect to the same reference frame. For a particle emerging from the target at (θ, ϕ), the differential cross section is modified according to

$$\sigma(\theta,\phi) = \sigma_{unp}(\theta)\,[1 + 2\ it_{11}\ iT_{11}(\theta) + t_{20}\ T_{20}(\theta) + 2\ t_{21}\ T_{21}(\theta) + 2\ t_{22}\ T_{22}(\theta)] \tag{23}$$

where the $T_{kq}(\theta)$ are the analyzing powers of rank k ($k = 1$ is vector, $k = 2$ is tensor) and the t_{kq} are the corresponding beam polarizations. They are given by

$$\begin{aligned} it_{11} &= \frac{\sqrt{3}}{2}\, p_Z\ \sin\xi\ \sin(\psi-\phi) & t_{20} &= \frac{1}{2\sqrt{2}}\, p_{ZZ}\ (3\cos^2\xi - 1) \\ t_{21} &= -\sqrt{\frac{3}{2}}\, p_{ZZ}\ \sin\xi\ \cos\xi\ \cos(\psi-\phi) & t_{22} &= \frac{\sqrt{3}}{4}\, p_{ZZ}\ \sin^2\xi\ \cos 2(\psi-\phi)\ . \end{aligned} \tag{24}$$

The small vertical spin component that signals the presence of an intrinsic EDM appears as a left-right asymmetry through the $it_{11}iT_{11}$ term because p_Z is large (~ 0.5) and $\psi - \phi = \pm\pi/2$ maximizes $\sin(\psi-\phi)$. This happens with opposite sign on the left and right sides of the beam when the vertical component makes $\psi = \pm\pi/2$. Such an asymmetry can also arise through the $t_{21}T_{21}$ term if $p_{ZZ} \neq 0$ and $\psi - \phi \sim 0$ or π. This situation arises naturally if the anomalous precession is not cancelled to extremely high precision. One can distinguish these two effects by allowing ω_a to act and measuring the polarization as a function of time. A Fourier analysis would separate the $\sin\xi$ from the $\sin\xi\cos\xi = (\sin 2\xi)/2$ dependence provided ξ was allowed to vary by a large enough angle such as π. In general, there are a number of systematic sources of a left-right asymmetry, such as a vertical polarization in the injected beam, misalignments of the beam at the polarimeter, non-linear detector response, and magnetic field errors that produce non-commuting rotations as the beam circles the ring. The Fourier analysis is crucial for extracting the $\sin\xi$ term associated with an EDM.

The polarimeter data from the EDM search consist of a set of deuteron polarization components measured as a function of the time during the store while the polarization slowly precesses ($\omega_a \neq 0$). The left-right asymmetry is only one of these components. The largest is the down-up asymmetry ($2it_{11}\langle iT_{11}\rangle \sim 0.4$) from the horizontal component of the vector polarization. The t_{22} tensor polarization produces another asymmetry that makes the sum of down and up rates different from the sum of left and right rates. This asymmetry is at a level below 0.01. There is a tensor contribution to the left-right (EDM) asymmetry that comes from the t_{21} beam polarization. Since we expect $T_{21}(\theta)$ to be a relatively small analyzing power in our case, this asymmetry enters at a level of 3×10^{-4}. While this is larger by at least an order of magnitude than the signal from an EDM at the 10^{-27} e-cm level, it has a period in ξ that is half that of the EDM signal. This may be used to

separate these contributions. As analysis of the EDM data requires the separation of these Fourier components, the EDM signal is more than a simple asymmetry. It is (1) a Fourier component associated with $\sin\xi$ whose size (2) varies as $\omega_{edm}/\sqrt{\omega_{edm}^2+\omega_a^2}$ and (3) has the correct behavior with respect to various reversals that are built into the running plan. These reversals include the change of the vector polarization sign (by solenoid field change or source RF transition), the change of beam revolution direction (CW or CCW), and the change of sign of the uncancelled anomalous precession (ω_a). Inherent in this scheme is the use of the down-up and tensor asymmetries to set the time when the polarization vector passes above or below the momentum direction so that the zero point for ξ is known. The systematic errors mentioned in the last paragraph produce signals that resemble an EDM signal in at most two of these three requirements. None satisfy all three.

In the region around 100 MeV the best sensitivity to vector polarization is associated with "rainbow scattering" [20], a phenomenon that generates iT_{11} analyzing powers that approach the maximum value of $\sqrt{3}/2$ starting at scattering angles larger than 20°. Because this effect comes from the action of the spin-orbit force between the deuteron and the nucleus, it is also present for most deuteron-induced inelastic and transfer reaction channels [21, 22]. Carbon is likely to be the best target since an extrapolation of the vector analyzing power among heavier mass targets at 200-MeV shows an increasing trend toward lower masses [23]. The rainbow scattering process allows for an open polarimeter geometry in which reaction products can easily exit the vacuum. Because the spin sensitivity extends to all reaction products, a detector system that surrounds the beam pipe works even without additional detectors for particle identification. The polarimeter analyzing power is the weighted average of iT_{11} for all particles that fall within the chosen detector acceptance and is expected to be at least 0.4.

The efficiency of the polarimeter needs to be be high. This requires carbon targets whose thickness is a significant fraction of the deuteron range in carbon (7.5 g/cm^3 for 126 MeV). To maintain compatibility with a continuously circulating beam, we will do "slow extraction" using a thin gas jet ($\sim 10^{15}$ /cm^2) to Coulomb-scatter deuterons onto a carbon target in the shape of a ring around the beam. This target is then the limiting aperture for the storage ring. The diameter of the opening in combination with the gas target thickness sets the beam lifetime.

One possible realization of the polarimeter is shown in Figure 2. To maintain symmetry for CW and CCW operation, the detectors are arrayed in a large disk built outside of the quadrupole (yellow box) that sits in the center of each straight section and are open to particles coming from either side. There is a movable carbon target (small magenta cylinder) located on either side of the detector array. The gas jets that illuminate the carbon targets are located farther away (red cylinder) on either side of the polarimeter.

The scattering and reaction data needed for the detailed polarimeter design are not available in the literature. Therefore we are planning to measure the cross section and iT_{11} for deuteron-induced scattering and reactions on carbon using the beam from the AGOR cyclotron at the KVI in Groningen. To confirm the design, a test of a prototype polarimeter is planned for the COSY ring at the KFA in Jülich.

3.3 Statistical Accuracy

An estimate of the time required to reach a sensitivity of 10^{-27} e·cm must consider that the beam itself is being used up and the polarization is decreasing exponentially. A simple estimate can be made for polarization that is initially fixed along the momentum of the beam. An optimization gives the best result for a measurement time that is equal to the polarization lifetime, and a beam lifetime that is half of the polarization lifetime. In this case the one standard deviation error on d

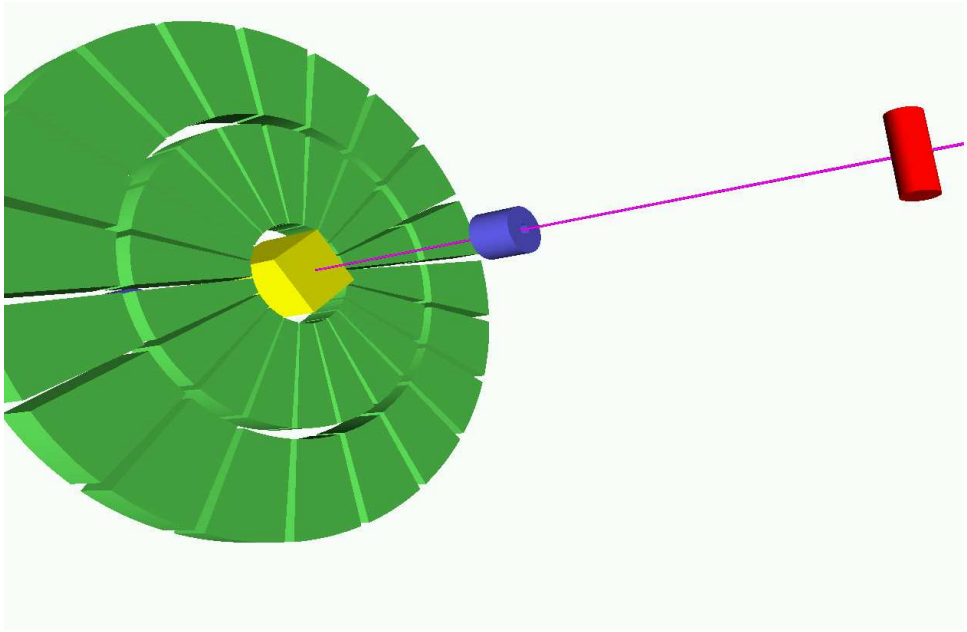

Figure 2: A schematic of the deuteron EDM Polarimeter.

is

$$\sigma_d \approx \frac{4\hbar}{\sqrt{\tau_p}\ (\beta c B_V - E_R)\ \imath t_{11}\langle \imath T_{11}\rangle\ \sqrt{N_c f T_{tot}}}\ . \tag{25}$$

For a ring with momentum $p = 0.7$ GeV/c and polarization lifetime[1] $\tau_p = 10$ s, we use $E_R = 3.5$ MV/m, $B_V = 0.21$ T, and $N_c = 10^{11}$ deuterons/fill. The polarimeter has an efficiency of $f = 0.01$ and an effective asymmetry of $2\,it_{11}\langle iT_{11}\rangle = 0.36$. The time needed to reach an error of $\sigma_d = 10^{-27}\,\mathrm{e}\cdot\mathrm{cm}$ is about $T_{tot} = 6 \times 10^5$ s, or just over one week of continuous operation.

We request running for 6 months for commissioning the ring and another 6 months for the first measurement. Most of this time goes toward the investigation of systematic errors. In particular, measurements will be made at different ring momenta and at multiple values of ω_a to learn whether the $\sin\xi$ Fourier component has a strength that varies as $\omega_{edm}/\sqrt{\omega_{edm}^2 + \omega_a^2}$. We wish to take this running time over a span of two years.

With 10^{11} deuterons/fill, the polarimeter rate is $\sim 10^8$ events/s. We will use use current-mode sampling as the method of detector readout. This method has worked well for recent parity-violation experiments where the asymmetry associated with the signal is small [24]. The choice of rainbow scattering as the spin-sensitive process means that the polarimeter can be designed so that all detected particles have some analyzing power that contributes to the statistics of the measurement.

[1]Even though in our ring design the spin coherence time is estimated to be > 100 s, here we are making the conservative assumption that it is only 10 s.

4 Deuteron Storage Ring

4.1 Lattice Design Considerations

The conceptual elements of the proposed EDM ring are given in Table 1 and Fig. 3. They are defined by the choice of deuteron momentum acceptable for efficient deuteron polarimetry, $p_D = 0.7$ GeV/c, the readily attainable magnitude of the electric field at the chosen 5 cm distance between electrodes, $E_R = 3.5$ MV/m, and the free space between lattice elements needed for the chosen number of polarimeters, 4. In addition, the CW-CCW procedure to cancel the E_V-field effect requires that the periodic sequence of the fields, $\vec{E}(s)$, $\vec{B}(s)$, met by the particles moving clockwise be the same as the periodic sequence of the fields, $\vec{E}(-s)$, $-\vec{B}(-s)$, met by the particles moving counterclockwise. The $\vec{E}$-field is always directed outwards. The minimization of the second-order perturbations imitating the EDM requires that the magnetic field, B_V, of any bending magnet not be separated in space from the radial electric field, E_R, in order to cancel the $g-2$ rotation in this magnetic field.

Table 1: Deuteron EDM ring parameters

Deuteron Momentum	0.7 GeV/c
Rigidity, $(B - E/\beta)R$	2.335 Tm
Electric field, E_R, for $2a_x = 5$cm	3.5MV/m (0.011667 T)
Magnetic field, B_V	0.2089 T
Length of orbit, L	155.28 m
$BE-$ section radius, R_0	13.302 m
Length of the $BE-$ section, l_{BE}	5.224 m
Number of regular periods, N	8
Horizontal tune, $\nu_x = \frac{f_x}{f_c}$	6.195
Vertical tune, $\nu_y = \frac{f_y}{f_c}$	5.810
Betatron amplitude functions, $(\beta_{x,y})_{\max}$	19.56 m; 21.91 m
Admittances, $\epsilon_{x,y} = \pi a_{x,y}^2/(\beta_{x,y})_{\max}$	32π mm mr; 28.5π mm mr
Momentum compaction factor, α	0.162
$(\Delta p/p)_{\max}$ at $x = 2.5$ cm	4.48×10^{-3}
Quadrupole gradient, B_g', for $l_g = 0.15$ m	311 Gauss/cm
Quadrupole focal length, f_q	5 m
Sextupole field derivatives, B_F'', B_D'', for $l_s = 0.3$ m	45 Tm^{-2}, 44.2 Tm^{-2}
Spin tune, ν_{sp}	$\sim 10^{-7}$
Number of Long Straight Sections, $N_{s.s.}$	4
Number of Free Intervals in One Straight Section	8
Length of a Free Interval, $l_{s.s.}$	1.2 m
Quadrupole gradients, B_{ss}' in s. Sections, for $l_{gs} = 0.366$ m	628.5 Gauss/cm
Sextupole derivatives, B_{ss}'', for $l_{s,sext} = 0.9$ m	-50.1 Tm^{-2}

Inside the BE sections, $B = B_V$ is homogeneous, while $E = E_R = E_0\frac{R_0}{R} = \frac{E_0}{1+x/R_0}$, where $R_0 = 13.302$ m is the designed radius of curvature of the BE sections, E_0 is the radial electric field at that radius, and $x = R - R_0$. In a linear approximation, the length of a particle path is proportional to $\frac{R}{R_0}$, $dl = (1 + \frac{x}{R_0})ds$, and the integrated electric fields met by the particles do not depend on transverse coordinates $(x,\ y)$. Therefore, the electric field does not influence betatron

focusing. The integrated electric potentials, however, and hence the full particle energy, depend on x; our design takes into account the corresponding small corrections of the betatron radial and synchrotron longitudinal frequencies.

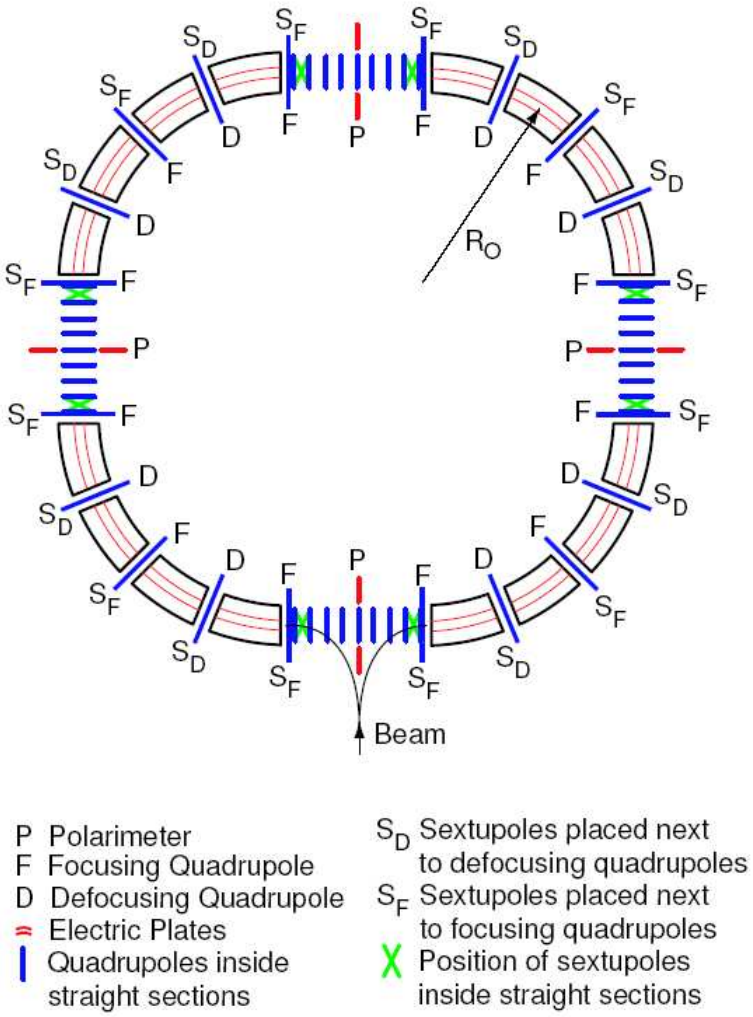

Figure 3: The deuteron EDM ring lattice.

Special care is taken with respect to the accuracy of the same absolute value of the vertical magnetic field, $|B_V|$, in CW vs. CCW runs. If $\delta B_V = |B_V|_{CCW} - |B_V|_{CW} \neq 0$, then the equilibrium radius, and hence the trajectory length of the CCW particles, differ from those of the CW particles,

$$\frac{\delta L}{L} = \left\langle \frac{\delta R}{R} \right\rangle = -\alpha \frac{\delta B_V}{B_V} \neq 0. \tag{26}$$

$\alpha = 0.162$ is the compaction factor from Table 1. Further, due to synchrotron stability, the revolution frequency, $f_c = \frac{\beta c}{L}$, is the same for CW and CCW particles. Therefore, a deviation

$\frac{\delta L}{L} \neq 0$ leads to the corresponding deviation,

$$\frac{\delta\beta}{\beta} = \frac{\delta L}{L} \neq 0. \tag{27}$$

This, in turn, leads to an error in the cancellation of the value of $\frac{E_V}{\beta\gamma^2}$ by the CW-CCW method,

$$\delta\left(\frac{E_V}{\beta\gamma^2}\right) \sim \left(\frac{E_V}{\beta\gamma^2}\right)\alpha\left(\frac{\delta B_V}{B_V}\right) \tag{28}$$

This error is easily controlled by our preliminary cancellations of the vertical electric field up to the level $E_V/E_R \leq 10^{-9}$, in every fill.

Specifically, we will measure the vertical component of the deuteron polarization during a single fill, and then correct E_V. In addition, we can use the fast preliminary cancellations of $\frac{\langle E_V\rangle}{E_R}$ by a resonance procedure. At the final step of this procedure, we will apply a small RF perturbation to the E-field electrodes with the frequency slowly moving in the direction of the vertical betatron frequency. Then we will correct the E_V-component in accordance with the observed vertical beam deviation.

Obviously, this technique needs devices permitting us to apply small RF perturbations, with the frequencies of betatron oscillations and their possible combinations, to every element of the lattice, as well as devices for precisely observing beam responses to these resonance perturbations.

An RF cavity is needed in our ring to increase the spin coherence lifetime. An energy loss of about 5 eV per turn is expected due to the presence of the gas jet in the beam path. This energy loss will be compensated for by the electric field in the RF-cavity. We have estimated that this effect requires the RF-cavity to be aligned with respect to the E-field plane at the 10^{-4} radian level, which is easily attainable. This effect changes sign going from CW to CCW, and hence it is mimicking the EDM signal. However it does not follow the same behavior as the EDM signal at different deuteron momenta.

4.2 Polarization Lifetime (Spin Coherence Time)

In our lattice design, the spin coherence time is greater than 100 s. During this time,

$$\omega_a = \frac{e}{m}\left[aB_V - \left(a - \left(\frac{mc}{p}\right)^2\right)\beta E_R\right] \tag{29}$$

is controllably small, $\omega_a \sim 0.1$ s^{-1}. With such a small ω_a, we have no spin resonances at the betatron and synchrotron frequencies. The undesirable depolarization effects are mostly caused by the spread of the particles' betatron and synchrotron deviations. In a linear approximation, in the commonly used notation,

$$x(s) = D(s)\frac{\Delta p}{p} + A_x\sqrt{\beta_x(s)}\cos\left(\psi_x(s) + \delta_x\right) \text{ , horizontal} \tag{30}$$

$$y(s) = A_y\sqrt{\beta_y(s)}\cos\left(\psi_y(s) + \delta_y\right) \text{ , vertical} \tag{31}$$

$$\frac{\Delta p}{p} = \left(\frac{\Delta p}{p}\right)_{max}\cos\left(\omega_L t + \delta_s\right) \text{ , momentum} \tag{32}$$

where s is the longitudinal coordinate, and the synchrotron frequency ω_L is much smaller than the betatron frequencies, $\nu_L << \nu_{x,y} \equiv f_{x,y}/f_C$. The Courant-Snyder betatron functions $\beta_{x,y}$ are given

in Table 1 in meters. The amplitudes $A_{x,y}$ are measured in $\mathrm{m}^{1/2}$, and when $x_{max},\ y_{max} \sim 2.5$ cm, $A^2_{x,y} \sim 30 \times 10^{-6}$ m. Due to betatron and synchrotron oscillations, all first order (linear) spin perturbations related to the spread of $x,\ y,\ \Delta p/p$ vanish on the average (in time) for every individual particle. Without the synchrotron RF, momenta do not oscillate ($\omega_L = 0$), and with the spread $|\frac{\Delta p}{p}| = 10^{-3}$, the beam is depolarized after 6 ms.

With RF cancellation of the first-order contributions to the depolarization, we turn to second-order effects. The biggest are the effects of the free betatron oscillations, with their amplitudes $A_x,\ A_y$. The quadratic effects of spin decoherence time and its extension in an electron-positron storage ring were investigated experimentally, and in part theoretically, in the Budker Institute [25, 26]. The results of our independent theoretical analysis are completely consistent with their experimental results, taking into account the difference between their electron-positron and our EDM deuteron storage rings. In our ring, if no special measures are taken, then the deviation $\Delta\omega_a$ of a particle having parameters $A_x,\ A_y,\ (\frac{\Delta p}{p})_{max}$, from the designed ω_a-value is given by

$$\frac{\Delta\omega_a}{e|a|\frac{B}{m}} \approx (0.33\,\mathrm{m}^{-1})A_x^2 + (0.27\,\mathrm{m}^{-1})A_y^2 + 1.26\left(\frac{\Delta p}{p}\right)^2_{max}, \tag{33}$$

$$\frac{e}{m}|a|B = 2\pi \times 143.93\,\mathrm{kHz}\,. \tag{34}$$

When maximal x and y equal 2.5 cm, and there is no momentum spread (while synchrotron stability is present), the spin coherence lifetime equals only 0.7 s. We cancel these "natural" effects by counter-effects, using the 0.3-m long sextupoles in the regular part of the lattice, and the 0.9-m long sextupoles inside the extreme left and the extreme right intervals of every long straight section. The sextupole parameters are given in Table 1. The long straight sections are introduced mostly for the purpose of this spin decoherence cancellation. In the beam (not spin) dynamics formalism, in the linear approximation, every straight section is equivalent to the identity matrix.

The cancellation of the quadratic terms proceeds as follows. Consider some oscillator with a quadratic nonlinearity,

$$\frac{d^2z}{dt^2} + \omega^2 z = kz^2. \tag{35}$$

The equilibrium position of this oscillator has the non-zero value $z = \langle z\rangle = k\frac{\langle z^2\rangle}{\omega^2}$, averaged over time. This fact lies at the basis of the idea of decoherence cancellation by quadratic fields. The vertical component of a sextupole field equals

$$\frac{1}{2}\frac{\partial^2 B_V}{\partial x^2}(x^2 - y^2). \tag{36}$$

Its horizontal component does not influence spin, on the average. The shift of the horizontal equilibrium, $\langle x\rangle \neq 0$, produced by such a field is proportional to

$$0.5B''\left(\langle x(s)^2\rangle - \langle y(s)^2\rangle\right) = 0.25B''(s)\left[\beta_x(s)A_x^2 - \beta_y(s)A_y^2 + D^2(s)\left(\frac{\Delta p}{p}\right)^2_{max}\right], \tag{37}$$

where all parameters are the same as in Eqs. (29)-(34). The equilibrium shift depends on a particle's parameters and changes the length L of the trajectory of this particle. Since the rotation frequency, $f_C = \beta c/L$, is fixed by the synchrotron stability, the particle momentum is changed. This shift of the equilibrium momentum shifts ω_a. In our design, this $\Delta\omega_a$ is opposite to the "natural" shift.

4.3 Non-Commutativity of Spin Rotations Imitating the EDM Rotation

At the very basis of a class of second-order effects imitating the EDM spin rotation lies the fact that rotations around different axes generally do not commute. If there is a set of consecutive rotations around different axes, that is, with different angular vectors, $\vec{\omega}_1 t_1$, $\vec{\omega}_2 t_2$, $\vec{\omega}_3 t_3$, $\vec{\omega}_4 t_4$, ..., and the sum $\Sigma \vec{\omega}_i t_i = 0$, (a closed loop), then the integrated spin rotation is *not* zero. In particular, if the closed loop of these vectors lies in a plane, then the spin is rotated around the axis perpendicular to this plane.

This is demonstrated in a simple and relevant example. Let $\delta_1 = \omega_a t_1 << 1$ be a small angle of rotation around the vertical axis due to a local deviation of ω_a from zero (due to, say, some level of the dipole magnetic field, ΔB_V, exceeding the designed value). Let $\delta_2 = \omega_L t_2 << 1$ be a small angle of rotation around the longitudinal axis due to some local longitudinal magnetic field, B_L. Last, let the restoring rotations be $\delta_3 = -\delta_1$, and $\delta_4 = -\delta_2$. From the linear equation for the spin, $d\vec{s}/dt = \vec{\omega} \times \vec{s}$, we can easily find the spin transition matrices for all four rotations, and their product M, keeping only up to second-order terms:

$$
\begin{aligned}
M \;=\; & \begin{bmatrix} \frac{1}{\sqrt{1+\delta_2^2}} & -\delta_2 & 0 \\ \delta_2 & \frac{1}{\sqrt{1+\delta_2^2}} & 0 \\ 0 & 0 & 1 \end{bmatrix} \times \begin{bmatrix} \frac{1}{\sqrt{1+\delta_1^2}} & 0 & -\delta_1 \\ 0 & 1 & 0 \\ \delta_1 & 0 & \frac{1}{\sqrt{1+\delta_1^2}} \end{bmatrix} \\
& \times \begin{bmatrix} \frac{1}{\sqrt{1+\delta_2^2}} & \delta_2 & 0 \\ -\delta_2 & \frac{1}{\sqrt{1+\delta_2^2}} & 0 \\ 0 & 0 & 1 \end{bmatrix} \times \begin{bmatrix} \frac{1}{\sqrt{1+\delta_1^2}} & 0 & \delta_1 \\ 0 & 1 & 0 \\ -\delta_1 & 0 & \frac{1}{\sqrt{1+\delta_1^2}} \end{bmatrix} = \begin{bmatrix} 1 & 0 & 0 \\ 0 & 1 & -\delta_1\delta_2 \\ 0 & \delta_1\delta_2 & 1 \end{bmatrix}
\end{aligned}
\tag{38}
$$

We see that the result of two small rotations and counter-rotations around the vertical and longitudinal axes is a quadratically small rotation around the radial axis.

Note that in our design, the E and B fields are combined at the same locations, so δ_1, δ_2, ... are very small. If this were not done, δ_1, δ_2, ... would be big and we would have additional first-order perturbations.

Examples of such δ_1, δ_2 errors include (1) longitudinal magnetic fields from bending magnet misalignment in the presence of a finite $g-2$ rotation, (2) longitudinal magnetic fields mixed with locally high and low values of the bending magnet field, and (3) a non-vanishing local $\vec{E} \cdot \vec{B}$ in the presence of a finite $g-2$ precession. All of these second-order systematics yield vertical polarizations that can be distinguished in data analysis from an EDM signal. The size of the resulting vertical polarization is independent of ω_a, unlike the EDM signal which varies with ω_a as in Eq. 1. To the extent that the components of the error cycle are spread out around the ring, polarimeters in different locations will record different results, unlike the EDM signal which is the same every where. In some cases, such as the error arising from $\vec{E} \cdot \vec{B} \neq 0$, the vertical Fourier component is $\cos\xi$ rather than $\sin\xi$. Thus in addition to minimizing the driving errors behind second-order effects, analysis signatures exist that can separate them from the EDM signal.

4.4 Magnetic/Electric Field Monitoring/Feedback Stabilization

In order to cancel the deuteron $g-2$ precession with a relative accuracy of 10^{-7} we need to control the *relative* values of the magnetic and electric fields at the same level. We will employ two ways determining the B and E fields to that precision: (1) by the deuteron $g-2$ (or horizontal) precession angle, and (2) by the Ramsey resonance technique using atomic and molecular beams.

(1) The statistical error in the determination of the horizontal spin precession angle is given by $\delta\omega_a = 2\sqrt{2}/(\tau\ it_{11} iT_{11}\ \sqrt{Nf})$, where τ is the beam lifetime, it_{11} and iT_{11} are the beam polarization

and analyzing power respectively, and f is the efficiency of the polarimeters. With a single store of 4×10^{11} polarized deuterons, it will be possible to determine the horizontal spin precession angle with a statistical error of the order of $10\,\mu$rad. Taking into account that π radians within a 10-s storage time would correspond to 10^{-7} relative stability between the B and E fields, it is obvious that the relative field knowledge from a single measurement will be of the order of 10^{-12}, much better than needed. This knowledge will be used to control ω_a with feedback to trim magnets and E field electrodes to the desired level.

(2) The electric field will be measured by using the Ramsey resonance technique in which we measure the splitting between the $J = 1$, $|M| = 0$ state and the $J = 1$, $|M| = 1$ states in a molecular beam of ^{206}Pb^{16}O. The ^{206}Pb^{16}O molecule is chosen because of its strong interaction with an electric field and its extremely weak interaction with a magnetic field. This allows for a direct probe of the electric field without the need to turn off the magnetic field. The technique described here will allow for continuous monitoring of the average value of electric field on a resonant signal that changes by one FWHM as the electric field changes by 2.4×10^{-2} V/m. If feedback is used to stabilize this resonance to 1% of its FWHM, we will be able to stabilize the average electric field to 2.4×10^{-4} V/m, or one part in 3×10^9, well within the 10^{-7} level requirement.

The technique will also allow for initial alignment of the angle between the electric and magnetic field. ^{206}Pb^{16}O represents an extreme case of sensitivity to electric field with little sensitivity to magnetic field. The Zeeman effect in atomic Li represents the opposite extreme of sensitivity to magnetic field with little sensitivity to electric field. By adding Li to the molecular beam, one would obtain a resonance (in the strong magnetic field limit) of 2.8 MHz/Gauss. Assuming one could resolve the width of the resonance to 1 Hz, the magnetic field could be stabilized to 10^{-6} G, or roughly one part in 10^{10}. Thus a combined molecular/atomic beam will allow for simultaneous stabilization of the electric and magnetic field magnitudes to one part in 3×10^9.

5 Systematic Errors

5.1 Systematic Errors due to Electric and Magnetic Field Imperfections

The dominant systematic error ($\simeq 10^{-27}\,\mathrm{e}\cdot\mathrm{cm}$) is due to $\langle E_V \rangle$, which we now discuss in detail. In a storage ring with only magnetic fields, a particle follows an orbit such that the average radial magnetic field is zero. Otherwise there is a net vertical Lorentz force, and the particle would not be stored. With an average vertical electric field $\langle E_V \rangle$, the storage requirement on the average vertical force is

$$\langle F_V \rangle = e(\beta c \langle B_R \rangle + \langle E_V \rangle) = 0 \tag{39}$$

This gives an average radial magnetic field in the particle's rest frame

$$\langle B_R^* \rangle = \gamma \left(\langle B_R \rangle - \beta \langle E_V \rangle / c \right) = \frac{\langle E_V \rangle}{c\beta\gamma} \tag{40}$$

which precesses the spin about the radial direction:

$$\omega_{E_V} = \frac{ge\langle E_V \rangle}{2mc\beta\gamma^2} \tag{41}$$

This is the only first order spin dynamics systematic error, i.e. this error by itself produces a systematic effect. The precession ω_{E_V}, relative to ω_{edm}, changes sign when injecting beam clockwise (CW) vs. counter-clockwise (CCW). The EDM signal is a difference in the measured deuteron

spin precession about the radial direction when injecting CW vs. CCW. Without this symmetry, $E_V/E_0 < 3 \times 10^{-13}$ would be required for an EDM systematic error of 10^{-27} e·cm.

The CW/CCW procedure will not perfectly cancel the $\langle E_V \rangle$ systematic error because:

1. The CW/CCW runs are taken at different times separated by $\simeq 30$ s.
2. The spatial extent of the beam will be different CW/CCW.
3. There may be systematic changes in E_V when the magnetic field is reversed during the CW/CCW procedure. Note that the electric field is not reversed during the CW/CCW procedure.
4. The magnetic field does not reverse perfectly CW/CCW.

We now discuss these in order.

1. Temporal stability of $\langle E_V \rangle$.

In order to evaluate the temporal stability, we have used our experience with the E821 storage ring. We found in E821 that the average radial magnetic field varied by $\simeq 10^{-5}$ of the main field over a period of about one month. Figure 4 shows the output of an inclinometer, with resolution about 10^{-10} radians, placed on the E821 magnet, along with the temperature readings, over a two day period. These measurements are consistent with our radial magnetic field variation experience; however the precision is much greater. There is a clear correlation with temperature. We plan better temperature control in the EDM experiment by a factor of about 4. These data give an imperfect cancellation from one 30s segment to the next equivalent to $\simeq 10^{-11}$ radians. Extrapolating from two days to 10^7 s data collection time gives a non-perfect cancellation equivalent to $\simeq 10^{-12}$ radians, where we have assumed for the purpose of this calculation that the non-perfect cancellation goes as $1/\sqrt{N}$. The next step is to build real electrodes and measure the temporal stability at many locations simultaneously with an interferometer described below, which has resolution of $\simeq 10^{-13}$ radians. From the present inclinometer data with four times better temperature stability, we thus estimate the EDM systematic error to be $\simeq 10^{-27}$ e·cm due to temporal variations CW/CCW.

2. Spatial reproducibility of the beam CW/CCW.

In order for the CW and CCW injections to cancel the systematic errors, the injected beam distribution needs to be "exactly" the same for CW and CCW. How "exactly" the same depends on the multipole content of the vertical electric field.

Computer simulation of the field of realistic electrodes using the 2-D computer program OPERA [27] were performed. The design was guided by the desire to reduce the dipole component of $E_{\rm V}$ as well as higher multipole components. The amplitudes of $E_{\rm V}$ compared to the radial E-field amplitude are all below 0.2 ppm as is shown in Table 2.

Table 2: $E_{\rm V}$ Multipoles at $R = 2$ cm from the center of the storage region normalized to the radial E-field.

N	0	1	2	3	4	5
$E_{\rm V}(N)/E_{\rm radial}$ [ppm]	0.01	0.2	0.07	0.06	0.005	0.005

The quadrupole component ($N = 1$) is equal to 0.2 ppm, i.e. 2×10^{-7} at $R = 2$ cm. Since the CW and CCW contributions need to cancel at the 0.3 prad level, the beam needs to repeat the

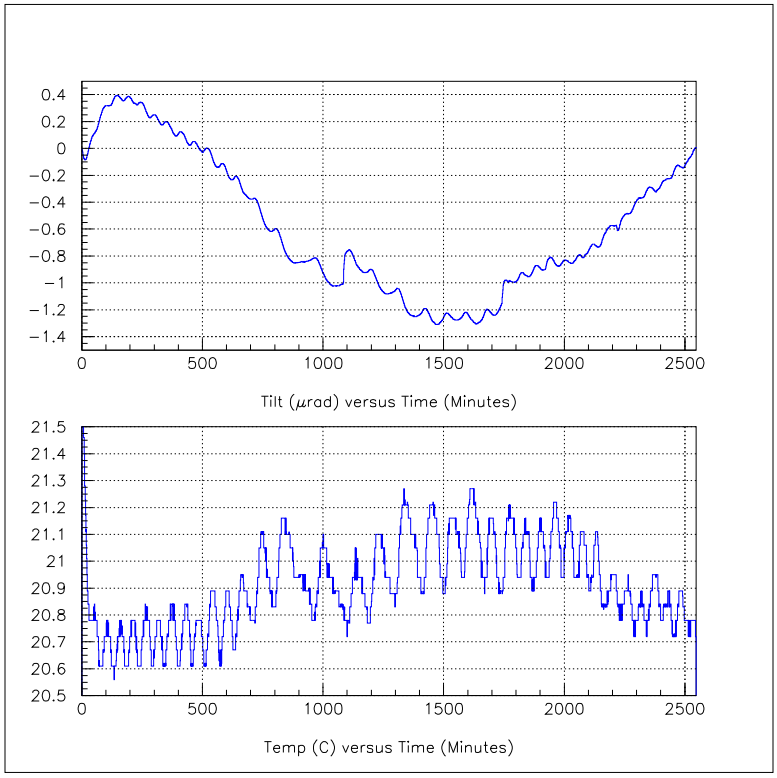

Figure 4: Tiltmeter data on top of the Muon $g-2$ ring magnet. The coordinates on the top figure are Tilt (in μrad) versus Time (in Minutes). The coordinates on the bottom figure are Temperature (in °C) versus Time (in Minutes).

average radial beam position to 30 nm, which can be measured with pickup electrodes. However, we plan to measure the $E_{\rm V}$ quadrupole component by moving the beam to about 1 mm larger radius and then apply a correction to a trim electrode. If we trim the field to 5%, the pickup electrode requirements will be much more relaxed. They would have to be able to measure the difference of the average beam position between CW and CCW of about 1 μm, which is already done in many storage rings.

The sextupole and higher order components of E_V couple to the same components of the beam and again need to be the same CW and CCW. The requirements for the pickup electrodes in these cases are more relaxed than the quadrupole component. We also plan to reduce further this problem by making the beam multipole content at least ten times larger [28] in order to obtain sensitivity to the multipole content of E_V. We then will minimize E_V with sextupole and other trim electrodes. Data taking will be done with the beam multipole contents minimized. The pickup electrodes, described in a later section, will monitor the beam multipole components throughout the experiment.

3. Systematic changes in E_V when the magnetic field is reversed during the CW/CCW procedure

To minimize the mechanical influence of the magnetic field on the electrostatic plates (ESP) the latter will be mounted independently of the magnet. The forces from the eddy currents on the vacuum chamber have been estimated to have a negligible effect on its mechanical stability. Even though the estimated effect from the magnetic field on the ESP orientation is expected to be below

the sensitivity of the deuteron experimental goal, it is nevertheless important to verify this with a measurement. For a 5-cm plate separation, 0.3 prad corresponds to 1.5×10^{-14} m shift in ESP, which is well within the capabilities of Fabry-Perot resonators using LIGO [29] techniques. The sensitivity level achieved at LIGO is more than 10^4 times better than our requirement at the 1-10 Hz frequency range. The idea is to install one mirror of the Fabry-Perot resonator on each plate of the ESP and test whether the plates move when the magnetic field value and/or its direction changes. This will first be performed on a test setup using up to a 1.5 T magnetic, greatly in excess of the ≈ 0.2 T field required for the actual experiment with deuterons.

Our collaborators from Italy (Legnaro and Trieste) have developed a very sensitive, high finesse, Fabry-Perot resonator [30] for the needs of the PVLAS experiment using technology similar to LIGO. Their Fabry-Perot resonator, with the addition of a reference laser cavity is expected to have the required sensitivity for our needs [31]. We expect this test to be the first we perform in the early stages of the experimental construction.

Another effect that could be different in going from CW to CCW is the so called patch effect or floating charges. The materials in the vicinity of the storage region could charge up during the deuteron storage time in which case the electric field would influence the stored beam. In order to avoid such a possibility the materials would need to be made of conducting metal and grounded. Even so a thin oxidized layer on their surface could develop with time. In the Berkeley Tl experiment the electric field plates were originally made out of Aluminium [32]. An oxidized aluminum layer developed which became a problem, because it acted like a high voltage insulator accumulating charge [32]. Their problems went away when they used Cu plates. The oxidized layer in Cu is conducting.

In our experiment we intend to use Cu metal when ever possible to minimize the patch effect. Special care will be paid to avoid backstreaming into the vacuum system from the vacuum pumps. Finally, the electrical charges accumulated due to a non-conducting layer will be mostly the same with CW and CCW injection.

4. Magnetic field does not reverse perfectly CW/CCW.

The presence of an EDM will cause the spin to develop a vertical component, i.e. the total spin precession plane will be off the horizontal plane. As can be seen from Eq. 1, when ω_a is not minimized, the influence of the EDM on the spin precession plane will be minimal while the contrary is true when ω_a is minimized. Therefore the EDM signal is the change of the spin precession plane between the following two running conditions: (1) the $g-2$ precession rate is minimized so that the deuteron spin is allowed to precess by about π rad within the 10 s storage period, and (2) the deuteron spin is allowed to precess 10π rad in a 10 s period. In order to be able to decipher the EDM effect, the B-field direction between the above two conditions can not be allowed to change more than that expected from the EDM effect itself.

With a 10^7 reduction of the $g-2$ precession, the ω_a rate will be of the order of 0.1 rad/s, i.e. 1 rad in 10 s. For a 10^{-27} e·cm deuteron EDM the spin precession rate ω_{edm} will be of the order of 0.3 μrad/s or 3 μrad in 10 s, i.e. the EDM at the above 10^{-27} e·cm level causes the spin precession plane to tilt by a little over 3 μrad.

However, the definition of "horizontal" might be subject to detector alignment and acceptance considerations. In order to define this plane uniquely for each polarimeter we will adjust the magnetic field, B, to cancel the $g-2$ precession at the 3×10^{-6} level. This allows the spin to make about five complete turns "horizontally". The tilt due to the EDM in this case is going to be small, less than 0.1 μrad, as is apparent from Eq. (19). Then to go to the 10^{-7} cancellation level we only need to change the amplitude of the magnetic field by about $\Delta B/B = 3$ ppm. We

can apply this extra magnetic field in the same direction as B to much better than 1 mrad so that the total B-field orientation will change less than 3 nrad, a much smaller change than the 3 μrad expected from the EDM effect.

In every CW injection we will have up to three runs, with variable control of the $g-2$ precession rate, so that at the end of the three 10 s running periods the spin will make about 5, 2 and 1/2 horizontal turns respectively. The difference of the spin precession plane between those running conditions will be uniquely determined for this CW injection. At the end of the above three runs we will go into CCW injection repeating the same running pattern. At the end of this operation we will compare the two sets of results. In simple terms, the sum corresponds to a background effect while the difference corresponds to a genuine EDM signal.

5.2 Polarimeter Systematic Errors

The vector left-right asymmetry that carries the EDM signal will be small in comparison to a number of other signals recorded by the EDM ring polarimeters. In order to separate this component from these other asymmetries, including systematic sources of a $\sin\xi$ term ($\xi = 0$ along the momentum direction), the measurement plan requires allowing some residual anomalous precession ($\omega_a \neq 0$) and a continuous measurement of the beam polarization during the store. With full azimuthal coverage, the polarimeters will also measure down-up asymmetries, a comparison of left and right with down and up that is sensitive to t_{22} polarization, and changes at large scattering angle in the azimuthally averaged rate that is sensitive to t_{20} polarization. If ω_a is stable during the store, one concept of the analysis would be to fit these asymmetries using a Fourier series based on $\xi = \omega_a t$ and extract the coefficient of the $\sin\xi$ term associated with an EDM. This coefficient would then have to have the right properties when certain experimental parameters are changed (spin-flip, sign of ω_a, beam revolution direction) as well as varying with ω_a as $\omega_{edm}/\sqrt{\omega_{edm}^2+\omega_a^2}$.

The data from the EDM search are binned according to value of ω_a for each store. The finite spread of ω_a values in each bin leads to an apparent depolarization that grows with time during the store. This is similar to the effect noted earlier that depolarizes the beam. Taking these together, the asymmetry exhibits a lifetime that must be included in the analysis model. Tensor polarizations decay twice as fast as vector [34].

To illustrate how the EDM signal can be separated from other sources of a left-right asymmetry, the table below lists a number of causes for an asymmetry and testable characteristics for each cause. A plus indicates that this cause appears to be the same as an EDM and a minus indicates where there is a distinguishable difference. The tests include "term," determining which term in the Fourier series would carry information on this cause, "spin-flip," the response to reversing the direction of the beam polarization, "sign ω_a," changing the direction of the anomalous precession, "mag. ω_a," measuring at more than one value of ω_a to learn whether the coefficient of the $\sin\theta_a$ term varies as $\omega_{edm}/\sqrt{\omega_{edm}^2+\omega_a^2}$ in Eq. (9), and "locat.," comparing results from more than one place in the ring. Lastly, an estimate is provided of the level at which the cancellation or the removal of this cause might be expected to fail. After the table, individual causes for left-right asymmetries are discussed in more detail. Here, items where distinguishability depends on experimental conditions (marked with an asterisk) are explained.

(1) A vertical polarization that is present when the beam is injected into the ring is constant independent of ω_a.

(2) Small tensor polarizations at the level of a few percent are expected from the ion source. With the polarization axis in the ring plane, a t_{21} tensor component generates a left-right asymmetry. The analyzing power $\langle T_{21}\rangle \sim 0.03$ is small because it is independent of the deuteron-nucleus

Table 3: Polarimeter Systematic Errors

ERROR	term	spin-flip	sign ω_a	mag. ω_a	locat.	CW/CCW	sens. ($e\cdot cm$)
(1) source p_y	$-$	$+$	$-$	$-$	$+$	$+$	$< 10^{-29}$
(2) source t_{21}	$-$	*	$+$	$-$	$+$	$-$	$< 10^{-29}$
(3) det. rotation	$+$	$+$	$-$	$-$	*	$+$	$< 10^{-29}$
(4) off axis/angle	$-$	$-$	$-$	$-$	*	$-$	$\sim 10^{-28}$
(5) non-linear det.	$+$	$+$	$-$	$-$	*	$+$	$< 10^{-29}$
(6) self-polarization	$-$	$-$	$+$	$+$	$+$	$-$	$< 10^{-29}$

spin-orbit force. But with p_{ZZ} only 0.02, the left-right asymmetry can be 4×10^{-4}, almost two orders of magnitude above our limit on an EDM signal. This term is eliminated in the Fourier analysis where it appears with half the period of the EDM signal. The response to spin-flip depends on the manner of generating the spin reversal. If the direction of the spin axis is changed at the spin precession solenoids in the beam injection line, the tensor polarization will remain the same and this term will not flip, thus contrasting it to a real EDM. If the switch is made at the ion source, the different hyperfine RF transition units used will introduce a different and unrelated tensor contamination of the beam.

(3) An error that could generate a "$\sin\xi$" Fourier coefficient would be any "rotation" of the detector boundaries that separate the down-up system from the left-right system. Since this effect is tied to the direction of the horizontal polarization component, it remains the same in the Fourier series analysis when ω_a is reversed, contrary to the EDM signal that changes sign. Additionally, this error is independent of the size of ω_a and may be different for different polarimeters in the ring.

(4) Left-right asymmetries can easily arise in polarimeters from small misalignments of the position or direction of the beam from the nominal center line through the polarimeter, or from some asymmetry in the efficiency of the detectors on the opposite sides, including their associated electronics and data acquisition logic. This commonplace error has typically been cancelled for many experiments by flipping the sign of the polarization of the beam, since these asymmetries do not depend on such changes. The analysis can be made more robust by considering "cross-ratios" that involve both left and right rates and both spin states [35]. If the left-right asymmetry is small (which it is), then corrections to the cross-ratio that depend on the derivatives of the analyzing power with angle appear at third order. For misalignments that are 1% of the distance to the detectors or 1% of a radian, these errors are less than 10^{-7} in the asymmetry or about $10^{-28}\,e\cdot cm$.

(5) Rates in the detectors are high, and photomultipliers as well as other systems are well known to have gains that depend on rate. These effects result in a detector response that, while it may depend linearly on rate over some operating range, is no longer proportional to rate. The rate in our system is an oscillation (on top of a constant or falling background) that comes from the spin precession. The largest effect is the down-up asymmetry that originates from the radial component of the deuteron spin, even if the detector is close to the plane of the storage ring. So long as the rate-dependent changes are in a linear range, only the magnitude of the asymmetry is affected. If the response contains a quadratic term and is different on the left and right sides, then this feeds into the $\sin\xi$ term in the Fourier analysis. As the stored beam loses intensity, the size of this term changes. Its dependence on ω_a will distinguish it from an EDM signal.

(6) Self-polarization of the beam is possible [36] since the ratio of the forward nuclear to the forward Coulomb amplitudes may have a significant magnitude when integrated over the acceptance

of the storage ring. This effect has not been observed and might appear for the first time in this experiment. Scattering spin-one deuterons from residual gas may introduce a t_{20} moment that smears into a t_{21} polarization (and a left-right asymmetry) as the spin precesses in-plane. This is the only systematic error that gets larger as ω_a gets smaller. It is distinguished by its Fourier signature and the fact that it is independent of the beam polarization. An important ancillary signature is a steadily rising t_{20} and t_{22} polarization.

All of these systematic effects that appear in the operation of the polarimeter, including those such as t_{21} and self-polarization that are unique to spin-one beams, are distinguishable from an EDM signal in at least two ways. It will be important that the analysis consider and model any effects that appear in the experiment at a measurable level. Otherwise, poor reproduction of the data will generate noise in the coefficient of the EDM term that will limit the sensitivity of the experiment.

5.3 Pickup Electrodes

The beam itself is the optimal tool for understanding the operational characteristics of the EDM storage ring, and this tool is made available with a system of Beam Position Monitors (BPM). A BPM system is an integral part of all storage rings. The BPM system is primarily used to determine orbit properties, but it can also allow the measurement of the beta-functions, the dispersion and the bunch length. The EDM storage ring will require beam position monitors in both the arcs and in the straight sections. The monitors are needed in the arcs to sense differences in the radial position of the beam for CW and CCW injection. A difference in the radial position between CW and CCW injection leads to a difference in average velocities, which, in turn, affects the accuracy of the cancellation of the vertical electric field. Since the required cancellation is 0.1 ppm and the bending radius is about 13 m, the *relative* beam position must be measured to the order of 1μm. The monitors are needed in the straight sections to sense changes in the beam position with respect to the polarimeters. Beam movement with respect to the polarimeter causes a false asymmetry. Since the expected asymmetry is 5×10^{-6}, the *relative* beam position here must also be measured to the order of 1μm. The number and position of the monitors will be better understood after measurements of field reversal accuracy on dipole and quadrupole prototypes have been made.

Beam position sensitivities of the order of 1μm have been achieved with pick-up electrodes. The typical configuration has two pairs of opposing conducting strips offset by 90°. Each strip subtends the same azimuthal width. The electric and magnetic fields of the circulating beam induce currents in the strips. The strips may be capacitively coupled to the beam line, in which case the BPM is an electrostatic device, or the strips may form with the beam pipe a transmission line with well defined impedance. While the fundamental limitation to these devices is the thermal noise power, the low signal levels (typically ~ 10 μV for ~ 1 mA of beam) requires careful exclusion of electromagnetic interference that is endemic to the accelerator environment.

6 Management

6.1 Group Organization and Responsibilities

The group has three spokespersons (Yannis Semertzidis at BNL, Jim Miller at Boston University, and Edward Stephenson at Indiana University) who share the responsibility for coordinating the activities of the collaboration. Changes to the management structure are voted by the entire collaboration. Activities to date have included planning, running calculations and simulations, and proposal preparation. If initial evaluations of this proposal are successful, then this same manage-

ment structure will provide the coordination for the preparation of a Technical Design Report and the start of "proof of principle" demonstrations of the performance of key ring, polarimeter, and diagnostic components. Measurements are expected to begin in the fall of 2004 (ahead of reviews) of the data needed for the design of the deuteron polarimeters. Financial coordination will be through BNL and/or the grants of individual investigators.

While BNL provides some attractive infrastructure in their accelerator complex, the low deuteron energy of the EDM ring would suggest that we consider other sites if a more cost effective experiment can be done there. We expect to solicit alternate proposals from the KVI in Groningen and from IUCF in Indiana. The collaboration will then appoint a sub-committee consisting of a representative from each bidding site and a chair from another institution to collect information on the bids and present a recommendation to the collaboration for a vote.

6.2 Outreach

The Deuteron EDM collaboration is committed to educating young people around the United States about the exciting challenges of physics that may represent physics beyond the standard model. We have devised a multi-plan approach that will not only be accessible to the entire population of the United States through web based material and an educational movie, but we will also identify school districts in each state that are generally not chosen to receive special attention.

We intend to develop a web site that explains the significance of the experiment in terms that the young children and non-scientists will be able to understand. This would be an avenue reaching individuals throughout the US, and the world. We intend to make the program user friendly, and will have an interactive link so that the physicists are able to answer questions from the individuals who access the web site.

We will prepare a documentary educational film about the EDM, its significance and the experimental effort, and distribute it to school districts that express an interest in learning more about the EDM. We will contact PBS or the Discovery Channel about participating in the production of the film, and about possibly airing the documentary film in order to create interest in the field of high-energy physics.

We intend to contact the Boards of Education in every state to inform them of the experiment and the significance of the EDM to the future of physics, and to make them aware of our programs aimed at educating children from kindergarten through 12^{th} grade. We will identify at least one school district in each state that we will pursue as a special school district so that the students will be aware of our experiment, the underlying science and its importance to the future of physics. These school districts will be those that are not consistently chosen for expanded educational opportunities. We will also identify the Science and Mathematics secondary schools in various states so that we can reach young people who have already expressed a desire to pursue scientific careers. In this way, we will reach the students who have committed themselves to the field, and possibly persuade them to choose high-energy physics as their area of expertise.

We will create a summer project for a few high school students and elementary school teachers who would work on the project during the summer. A physicist would visit the school in the fall as the student or teacher gives a presentation about what they learned during the summer in order to interact with all of the students and to answer their questions.

Scientists who were educated in the United States and are working on the EDM will visit the grade school, middle school and high school that they attended, and spend a day with the students and teachers. They will present information about the EDM, and allow time for the students to ask questions.

The costs for outreach that will be carried by the grant are summarized in Table 5.

Table 4: Outreach Costs

Description	**Cost Rate**	Total Cost[1]
Full Time Outreach Manager	\$80 K[2]	\$480 K
3 Summer Program Teachers	\$6 K/month	216 K
12 Summer Students	2.5 K/month	\$360 K
	Total	**\$1056 K**

7 Cost and Schedule

After the proposal is successful, we expect to complete a Technical Design Report (TDR) in roughly six months. After a successful review of the TDR we will work on the proof of principle of the Fabry-Perot resonator to achieve the required level of accuracy. In parallel we will be developing the design of the E-field plates and demonstrate the proof of principle by operating them at full voltage in the required magnetic field. With the Fabry-Perot resonator we will have to show that reversing the B-field does not influence mechanically the E-field plates at the required level.

At the same time we will be further developing spin and particle tracking programs to guide the design of the deuteron EDM storage ring. We expect to be ready to start the ring construction in three years after the approval of the proposal. The ring construction will take two years to complete at the end of which we would be ready to take beam. The first year we will have an engineering run to shim the B and E-fields and to achieve the required deuteron spin coherence time. During the second year we will be ready for a physics run. We thus expect to have taken the required data by the end of 2010.

The estimated construction costs for an experiment to search for the EDM of the deuteron in a storage ring at BNL is given in the following table.

7.1 Conventional Facilities

Description		**Cost**
Beam transport shielding		\$240 K
30 m diameter storage ring shielding		1,286 K
Entrances & exits		80 K
Power substation		250 K
Cooling tower upgrade		100 K
Support Buildings		100 K
	Sub-Total	**\$2,056 K**
	Including Burdens [1]	**\$6,051 K**

7.2 Accelerator Modifications

New RFQ cavity		430 K
Spin rotators for LEBT and MEBT		\$222 K
	Sub-Total	**\$652 K**

7.3 Beam Transport

Magnets & power supplies [2]		\$0 K
Vacuum		\$200 K
Controls		50 K
Instrumentation		100 K
Spin Precession Solenoids		
	Sub-Total	**\$350 K**
	Including Burdens	**\$1,030 K**

7.4 Storage Ring

16 dipole magnets @ \$50 K each		\$800 K
48 quadrupole magnets @ \$25 K each		1,200 K
32 sextupole magnets @ \$15 K each		480 K
Dipole power supply		250 K
Quadrupole magnet power suppply		250 K
RF cavity & associated equipment		75 K
Vacuum & vacuum instrumentation		1,100 K
16 electric field regions with power supplies		1,500 K
Controls		240 K
Beam Instrumentation		500 K
	Sub-Total	**\$6,395 K**
	Including Burdens	**\$18,800 K**
Injection kicker magnet & PFN		2,123 K
	Sub-Total	**\$20,923 K**

7.5 Experimental Systems

Tiltmeters	100K	
Fabry-Perot Interferometers	300K	
Molecular Beams	1000K	
4 Polarimeters including data acquisition system.		\$929 K
8 Gas Jet Targets		2,950 K
	Sub-Total	**\$5,279 K**

7.6 Totals

\$33,935 K

[1] Costs for labor (75%), EDIA (Engineering,Design, Installation and Assembly) (15%), contingency (25%) and additional charges (17%) are each applied to the sum of the preceding costs. Total costs for items without the indication 'Including Burdens' were based on estimates from known costs including burdens based on recent experience with sufficiently similar devices.

[2] There is no charge for transporting magnets and power supplies which are assumed to be in stock.

7.7 R&D Request

Tiltmeters		20K
Fabry-Perot Interferometers		70K
Electrostatic Plates		50K
Molecular Beams		200K
Support for experts		25K/year×2y=50K
	Sub-Total	**$390 K**
	Including Burdens	**$1170 K**

This cost estimate was prepared for building the deuteron EDM storage ring at BNL. Other sites, such as the Indiana University Cyclotron Facility (IUCF) and the Kernfysisch Versneller Instituut (KVI) in Groningen, the Netherlands, are under consideration. Cost estimates will likely differ because of differences in the overhead rates, the amount of existing equipment and infrastructure that can be made available, and operating costs.

8 Conclusion

We propose a search for a deuteron EDM at the 10^{-27} e·cm level. At this level we will be sensitive to a non-zero deuteron EDM value predicted by a number of theories beyond the SM. The strength of the method resides in the following features:

- The $g-2$ precession can be reduced to the required 10^{-7} level.
- Our storage ring design makes possible spin coherence times greater than 10 s.
- High intensity (4×10^{11} per cycle), highly polarized deuteron beams are readily available.
- Polarimeters with high analyzing power (0.5) are available in the energy range of interest.
- Potential systematic errors can be corrected by polarization measurements of counter-rotating stored beams and polarization reversals.

The successful conclusion of this experiment will constitute a major advancement in the quest of finding a non-zero EDM for a fundamental particle.

References

[1] J.H. Smith, E.M. Purcel, and N.F. Ramsey, Phys. Rev. **108**, 120 (1957).

[2] R.L. Garwin and L. Lederman, Nuovo Cimento **11**, 776 (1959).

[3] J. Bailey, *et al.,* J. Phys. **G4**, 345 (1978).

[4] F.J.M. Farley *et al.*, Phys. Rev. Lett. 93, 052001 (2004); hep-ex/0307006.

[5] D.F. Nelson, A.A. Schupp, R.W. Pidd, and H.R. Crane, Phys. Rev. Lett. **2**, 492 (1959).

[6] P.G. Harris et al., Phys. Rev. Lett. 82, 904 (1999).

[7] B.C. Regan *et al.,* Phys. Rev. Lett. **88**, 071805 (2002).

[8] M.V. Romalis *et al.,* Phys. Rev. Lett. **86**, 2505 (2001).

[9] V.F. Dmitriev and R.A. Sen'kov, Phys. Rev. Lett. 91, 212303 (2003).

[10] O. Lebedev, K.A. Olive, M. Pospelov and A. Ritz, Phys. Rev. D **70**, 016003 (2004), hep-ph/0402023.

[11] A.D. Sakharov, JETP Lett., **5**, 24 (1967).

[12] J. Hisano and Y. Shimizou, hep-ph/0406091.

[13] J. Hisano *et al.,* hep-ph/0407169.

[14] C.P. Liu and R.G.E. Timmermans, KVI internal report: KVI-1660, (2004).

[15] I.B. Khriplovich and R.V. Korkin, Nucl. Phys. A **665**, 365 (2000).

[16] D. Demir *et al.*, hep-ph/0311314.

[17] N.F. Ramsey, Annu. Rev. Nucl. Part. Sci. 1990. 40:1-14.

[18] J.D. Jackson *Classical Electrodynamics* John Wiley and Sons, Inc.

[19] A. Silenko *et al.*, January 9, 2003. It can be found at "http://www-ps.kek.jp/jhf-np/LOIlist/pdf/L22.pdf" and from our own web site "http://www.bnl.gov/edm/". J-PARC: Japan Proton Accelerator Research Complex, "http://j-parc.jp".

[20] E.J. Stephenson, C.C. Foster, P. Schwandt, and D.A. Goldberg, Nucl. Phys. **A359**, 316 (1981).

[21] H. Sakai *et al.*, Phys. Rev. Lett. **44**, 1193 (1980).

[22] E.J. Stephenson *et al.*, IUCF Sci. and Tech. Report - 1981, p. 95.

[23] Nguyen van Sen *et al.*, Nucl. Phys. **A464**, 717 (1987).

[24] see T.M. Ito *et al.*, Phys. Rev. Lett. **92**, 102003 (2004) and references therein; also K.A. Anoil *et al.*, Phys. Rev. Lett. **82**, 1096 (1999).

[25] I.B. Vasserman *et al.*, Phys. Lett. B **198**, 302 (1987).

[26] A.P. Lysenko, A.A. Polunin, and Yu.M. Shatunov, Particle Accelerators **18**, 215 (1986).

[27] `OPERA`, Electromagnetic Fields Analysis Program, Vector Fields Ltd., 24 Bankside, Oxford OX5 1JE, England.

[28] T. Roser, private communication.

[29] http : //www.ligo.caltech.edu/

[30] A.M. De Riva, et al., Rev Sci. Instrum. 67, 2680 (1996) "Very high Q frequency-locked Fabry-Perot cavity". The actual length of the Fabry-Perot resonator used in the PVLAS experiment is 6.4m long, while the length of a test resonator they used was 1.7m long.

[31] G. Cantatore, private communication.

[32] E. Commins, private communication.

[33] Review of Particle Physics, Phys. Rev. D **66**, 1 (2002).

[34] B. von Przewoski *et al.*, Phys. Rev. E **68**, 046501 (2003).

[35] G.G. Ohlsen and P.W. Keaton, Jr., Nucl. Instrum. Methods **109**, 41 (1973).

[36] V.G. Baryshevski, LANL/Cornell archive hep-ph/0109099; hep-ph/0201202.